

## Space-charge-limited photocurrent transients: The influence of bimolecular recombination

G. Juška, M. Viliunas, and K. Arlauskas

*University of Vilnius, Sauletekio al. 9, III.k., 2054 Vilnius, Lithuania*

J. Kočka

*Institute of Physics, Cukrovarnická 10, 162 00 Prague 6, Czech Republic*

(Received 20 June 1994; revised manuscript received 30 December 1994)

Recently we presented a detailed theory of the space-charge-limited current (SCLC) transients generated by an instantaneous pulse of light, in which the realistic absorption profile has been taken into account. In this paper we present a theory that, in addition, takes into account the bimolecular recombination and the value of the detection resistor. This allowed us to propose a convenient method to study the fast recombination by electrical instead of the usual optical techniques. The method allowed us to present experimental results related to subnanosecond nonradiative bimolecular recombination in amorphous hydrogenated silicon (*a*-Si:H) and to discuss the microscopic origin of bimolecular recombination. The importance of understanding bimolecular recombination in *a*-Si:H is underscored by the fact that bimolecular recombination is the driving force of *a*-Si:H degradation.

### I. INTRODUCTION

In a time-of-flight (TOF) experiment, usually one surface of the sandwich sample is illuminated by a strongly absorbed light and a resulting current transient is studied. When we use the high light pulse intensity in the case of the space-charge-limited current (SCLC), the charge reservoir<sup>1</sup> with a high density of charge carriers is created. The time necessary to extract these carriers is the so-called extraction time ( $t_e$ ), see below. One of the factors that can seriously influence the extraction time and the shape of the SCLC transient is the recombination of the photogenerated carriers. The shape of the SCLC-TOF transients was used for the study of recombination already in iodine crystals.<sup>2</sup> Recently, SCLC-TOF studies led to conclusive evidence that in amorphous selenium the recombination is controlled by the Langevin-type mechanism.<sup>3</sup>

In a recent paper,<sup>4</sup> a detailed theory of SCLC transients was presented in which the realistic absorption profile of the pulsed light and the monomolecular recombination in the charge reservoir were taken into account. Moreover, it was shown<sup>4</sup> how the recombination time can be deduced from the measured extraction time. On the basis of the detailed theory<sup>4</sup> and further experimental results, it was found that the so-called integral mode of the SCLC-TOF transients is the most promising,<sup>5</sup> even for the study of the real solar cells on the basis of amorphous hydrogenated silicon (*a*-Si:H).

In a standard differential (so-called "current") mode of the TOF, defined by a condition  $t_{tr} > \tau_{RC}$  (where  $t_{tr}$  is the small charge transit time and  $\tau_{RC}$  the time constant of the measurement circuit), the SCL extraction current is a function of light intensity and volume trapping, which influences the extraction time. This complicates the

determination of recombination parameters.

In an integral mode ( $t_{tr} < \tau_{RC}$ ), the extraction current is controlled by the value of the detection resistor ( $R$ ) and the influence of trapping is minimized. (Note that even using  $R = 50 \Omega$  for most of *a*-Si:H solar cells the integral mode is the only possible mode of TOF.)

However, due to the high intensity of the pulsed light (typical of SCLC-TOF conditions) even in this case and, namely, for high-quality *a*-Si:H structures (solar cells), the influence of the fast bimolecular recombination cannot be neglected. Unfortunately, at present, the microscopic origin of this free-carrier controlled subnanosecond nonradiative recombination is not fully clear.<sup>6</sup> Although there are a few models, each of them has some serious difficulties.

On one hand, the bimolecular recombination complicates the application of SCLC-TOF transients for the evaluation of density of states on real *a*-Si:H solar cells.<sup>5</sup> On the other hand, the integral mode SCLC-TOF technique represents a method for studying the bimolecular recombination in *a*-Si:H. Recent preliminary results<sup>7</sup> demonstrated the advantages of this technique in comparison with the usual optical measurements, which are the following.

(i) The measurement of the extraction time by SCLC-TOF is carried out on the ns time scale, although the recombination starts on the ps time scale. (We can say with a certain simplification that we detect the remaining amount of carriers.) In comparison with the optical pump-and-probe techniques, much simpler equipment can be used.

(ii) In optical measurements, it is difficult to distinguish between the losses of the free carriers by recombination and by shallow trapping. In our case, the shallow-trapped carriers are extracted, too.

(iii) Our measurement can be carried out in a single-pulse mode, while for the optical methods, the high repetition rate is typical, which can lead to sample degradation.

(iv) In our case, it is possible to investigate the recombination of electrons and holes separately.

In this paper, after a brief description of the samples used and the TOF technique (Sec. II), we present (Sec. III) the detailed theory of the SCLC-TOF transients, generated by an instantaneous light pulse, in which in addition to the realistic absorption profile,<sup>4</sup> the bimolecular recombination and different values of the detection resistor are also taken into account. Then (Sec. IV), we illustrate the theory by using a few specific examples for both differential and integral mode SCLC-TOF and compare the calculated results with the experimentally observed ones. As a next step, we present the simplified theory (Sec. V), which allows us to find the simple analytical relation between the extraction time and the coefficient of the bimolecular recombination, and illustrate good agreement with the detailed theory. Then, we compare (Sec. VI) the simplified theory with experimental results. Finally, we discuss the data of other authors, different models of the microscopic origin of the bimolecular recombination in *a*-Si:H, present the temperature dependence of the bimolecular recombination, test its sensitivity to the degradation of *a*-Si:H, and test short-living states. The data allowed us to formulate our microscopic model of the bimolecular recombination in *a*-Si:H.

## II. EXPERIMENTAL DETAILS

The detailed theory described in the next section has been compared with the experimental results, which were obtained on different *a*-Si:H-based *p-i-n* junctions. We used device-quality *a*-Si:H *p-i-n* junctions with thickness ranging from 1 to 50  $\mu\text{m}$ . Thick *p-i-n* junctions are necessary when the differential (current) mode TOF is wanted. For the TOF experiment, the pulsed YAG:Nd (where YAG is yttrium aluminum garnet) laser with a half-width of 15 ps and a photon energy of 2.3 or 3.45 eV has been used. For these photon energies, the absorption coefficient of *a*-Si:H is  $\alpha \approx 10^5 \text{ cm}^{-1}$  (for 2.3 eV) and  $\alpha \approx 10^6 \text{ cm}^{-1}$  (for 3.45 eV). For the detection of TOF transients, an oscilloscope, able to record single-shot transients up to the 6-GHz range, has been used. The samples were placed at the end of the coaxial line<sup>3</sup> in a special sample holder, in which the temperature could be changed from 100 to 440 K.

## III. THEORY

In this section, we present the theory of SCLC-TOF transients generated by an instantaneous light pulse in which, in addition to the realistic absorption profile,<sup>4</sup> a bimolecular recombination and different values of the detection resistor ( $R$ ) are also taken into account. As in Ref. 4, we use the method of characteristics.

As in the standard SCLC theory,<sup>8</sup> in an effort to simplify the calculation we use the following well substantiated assumptions: (i) At time  $t=0$ , the electric field ( $E$ ) is homogeneous within the sandwich sample. We can

solve only the one-dimensional case for coordinate  $x$ . (ii) The sample is an insulating photoconductor, which means that we neglect the thermal carriers. (iii) Only carriers of one polarity (positive for mathematical simplicity) can move. The change of shape of the current transient when carriers of both polarities can move is discussed in Ref. 4. The influence of the less-mobile carriers in the integral mode of SCLC-TOF is less pronounced than in the current mode. (iv) The diffusion and trapping of the carriers are neglected.

To simplify the notation of equations we have used the same dimensionless (normalized) units as in Ref. 4. The coordinate  $x$  is normalized to the sample thickness (interelectrode distance  $d$ ,  $x'=x/d$ ); the time  $t$  is normalized to the small signal transit time,  $t'=t/t_{\text{tr}}$ ; the electric field to the initial field,  $E'=Ed/U$ , where  $U$  is the applied plus internal voltage. The surface density of the photogenerated electron-hole pairs ( $L$ ), electron ( $n$ ), and hole ( $p$ ) volume concentrations are normalized to the charge on the electrodes,  $L'=(Led)/(\epsilon\epsilon_0 U)$ ,  $n'=(ned^2)/(\epsilon\epsilon_0 U)$ , and  $p'=(ped^2)/(\epsilon\epsilon_0 U)$ .

In this case, the coefficient of the bimolecular recombination ( $B$ ) is normalized to the diffusion-controlled Langevin-type recombination coefficient  $B'=(B\epsilon\epsilon_0)/e\mu$ , where  $\mu$  is the mobility; current ( $j$ ) to the SCLC value  $j'=(jd^3)/(\epsilon\epsilon_0\mu U^2)$  and the optical absorption coefficient to  $1/d$ ,  $\alpha'=ad$ . The external circuit (detection) resistance (which also includes the possible contact electrode resistance) is given by the condition that  $R'=1$  when  $t_{\text{tr}}=\tau_{RC}$ .

With the above notation, the initial conditions are

$$E'(x',0)=1, \quad (1)$$

$$n'(x',0)=p'(x',0)=L'\alpha'\exp(-\alpha'x'), \quad (2)$$

and the boundary conditions

$$\int_0^1 E'(x',t')dx'=U'(t'). \quad (3)$$

Note that the condition  $U'(t')=1$  defines the current mode, as described in Ref. 4.

The total current equation is now expressed as

$$\begin{aligned} j'(t') &= p'(x',t')E'(x',t') + \frac{\partial E'(x',t')}{\partial t'} \\ &= \frac{dE'(0,t')}{dt'} = \frac{1-U'(t')}{R'}, \end{aligned} \quad (4)$$

the Poisson equation as

$$\frac{\partial E'(x',t')}{\partial x'} = p'(x',t') - n'(x',t'), \quad (5)$$

and the kinetic equation for the staying carriers, controlled contrary to Ref. 4 by the bimolecular recombination

$$\frac{\partial n'(x',t')}{\partial t'} = -B'n'(x',t')p'(x',t'). \quad (6)$$

On the basis of Eqs. (4)–(6) and initial and boundary conditions (1)–(3), we have found the following expression for the electric field:

$$\begin{aligned} & \frac{\partial E'(x', t')}{\partial x'} + \frac{1}{E'(x', t')} \frac{\partial [E'(x', t') - E'(0, t')]}{\partial t'} \\ &= \frac{d[E'(x', t') - E'(0, t')]}{dx'} \\ &= -\alpha' L' [E'(x', t')]^{B'} \exp(-\alpha' x') \exp(-A), \end{aligned} \quad (7)$$

where

$$A = \frac{B'}{R'} \int_0^{t'} \frac{1 - U(t')}{E'(x', t')} dt'.$$

The left-hand side of Eq. (7) represents the total differential of the electric field on the trajectory of the mobile carrier at the position  $x'(t')$ , given as

$$x'(t') = x'_0 + \int_0^{t'} E'(x' t') dt', \quad (8)$$

which started at  $t'=0$  at the coordinate  $x'_0$ .

From the computer simulations of Eqs. (7) and (8), we have obtained the electric-field distribution in the region through which the mobile carrier moved. The value of the electric field in the region from  $x'=0$  to the coordinate of the "last" mobile carrier, which started at  $x'_0=0$  (the "zone free from mobile carriers," see Ref. 4), is given by the screening of the field by immobile carriers, which escaped the recombination. It means that the recombination at coordinate  $x'$  is stopped when the last trajectory of the carrier, which started at  $x'_0=0$ , crossed  $x'$ . Further increase in the electric field, given by the supply of the charge from the voltage source according to Eq. (4), is the same as for  $E'(0, t')$  in this region; its value can be deduced from the boundary conditions [Eq. (3)]. Therefore, we can obtain the voltage on the sample electrodes and the current for each time  $t'$ .

#### IV. SPECIFIC EXAMPLES CALCULATED ON THE BASIS OF THE ABOVE THEORY

Figure 1(a) shows the SCLC-TOF transients for different light intensities calculated on the basis of Eqs. (7) and (8) in the differential mode for  $R'=0.1$  (i.e.,  $RC=t_{tr}/10$ ). The comparison of these results with the experimental results obtained on a 50- $\mu\text{m}$ -thick  $a\text{-Si:H}$   $p\text{-i-n}$  junction and displayed in Fig. 1(b) clearly demonstrates very good agreement.

Figure 2(a) shows the SCLC-TOF transients for different light intensities calculated for the integral mode ( $R'=10$ , i.e.,  $RC=10t_{tr}$ ) under otherwise identical conditions ( $\alpha'=30$  and  $B'=10^{-2}$ ). Again the experimental results obtained in this case on a 1- $\mu\text{m}$   $a\text{-Si:H}$   $p\text{-i-n}$  junction and displayed in Fig. 2(b) for both the small signal ( $L' \ll 1$ ) and the SCLC case ( $L' \gg 1$ ) agree qualitatively very well.

When we compare the differential and the integral modes of TOF [see Figs. 1(a) and 2(a)] we can see that, contrary to the differential mode, in the integral mode with the increasing light intensity ( $L'$ ) the length and the shape of the current transient clearly saturate.

In the current mode, the current for  $t < t_e$  is controlled by the space charge. It means that in the case of volume trapping, the current will decrease with time and this will increase the extraction time  $t_e$ . Moreover, with the in-

creasing light intensity the effective thickness  $d'_{\text{eff}} = 1 - (\ln L' / \alpha')$  decreases, leading to an increase in the current above the value of the standard SCLC.<sup>4</sup> Naturally this will also change the value of  $t_e$ .

The above problems are absent in the integral mode in which the extraction current is given mainly by the external (detection) resistor. In Ref. 7, we have suggested a definition of the extraction time  $t_e$  as the difference between the half-width of the current transient at the high and low intensities of light (see Fig. 3)

$$t'_e = t'_{1/2}(L' > 1) - t'_{1/2}(L' \ll 1), \quad (9)$$

which is substantiated by the fact that

$$t'_{1/2}(L' \ll 1) = \frac{1}{2} + R' \ln 2,$$

$$t'_{1/2}(L' > 1) = C + t'_e + R' \ln 2 \quad \text{for } L' > 1,$$

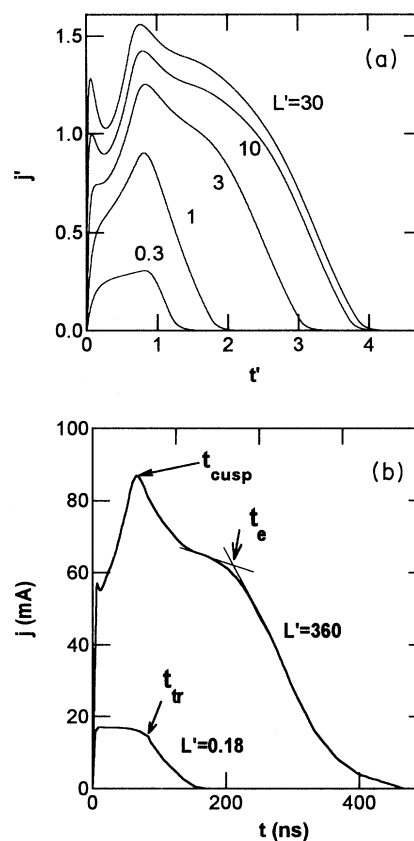


FIG. 1. (a) The SCLC transients in the current mode of TOF (for  $R'=0.1$ ), calculated for different values of the light intensity ( $L'$ ). Current ( $j'$ ), time ( $t'$ ),  $L'$ ,  $R'$ , and other parameters ( $\alpha'=30$  and  $B'=10^{-2}$ ) are used in normalized units. For their definitions, see text. (b) The current transients measured at 300 K and a voltage of 700 V applied across a 50- $\mu\text{m}$ -thick  $a\text{-Si:H}$   $p\text{-i-n}$  junction in the so-called small signal case ( $L'=0.18 < 1$ ) and at the saturated (high light intensity) value of  $L'=360$ . The detection resistor  $R=50 \Omega$  was used and for the used wavelength the absorption coefficient of  $a\text{-Si:H}$  is assumed to be  $\alpha=10^5 \text{ cm}^{-1}$ . The  $t_{tr}$  is the small signal transit time and  $t_e$  is the charge reservoir extraction time (see text).

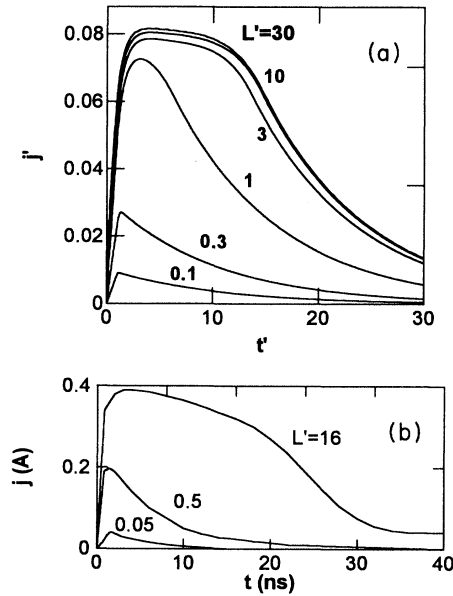


FIG. 2. (a) The SCLC transients in the integral mode of TOF (for  $R'=10$ ), calculated for different values of the light intensity ( $L'$ ). Except  $R'$  the other used parameters ( $\alpha'=30$ ,  $B'=10^{-2}$ ) are the same as in Fig. 1(a). (b) The current transients measured at 300 K and 23 V applied across a 1- $\mu\text{m}$ -thick  $\alpha\text{-Si:H}$   $p\text{-i-n}$  junction in the small signal case ( $L'=0.05$  and  $L'=0.5$ ) and at the saturated (high light intensity) value of  $L'=16$ . As in Fig. 1 (a),  $R=50\ \Omega$  and  $\alpha=10^5\ \text{cm}^{-1}$  were used.

where constant  $C$  varies as a function of  $\alpha'$  and  $L'$  in the range  $C \leq 1$ .<sup>3</sup>

Clear saturation of  $t'_{1/2}$  with the increasing light intensity is illustrated by points in Fig. 3, which represent the  $t'_{1/2}$  values taken from Fig. 2(a), calculated on the basis of Sec. III. The full line was calculated on the basis of the simplified theory of Sec. V. The magnitude of the current pulse [see below, Fig. 6(b)] is a linear function of  $L'$  for

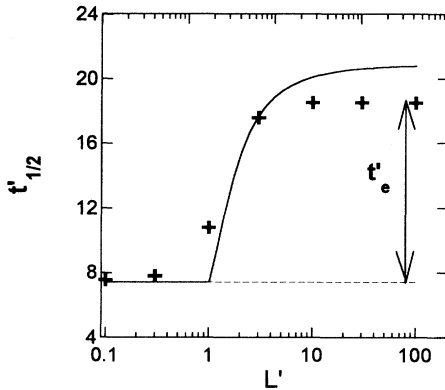


FIG. 3. The SCLC-TOF current pulse half-width ( $t'_{1/2}$ ) as a function of the light intensity ( $L'$ ). The points have been calculated from the transients in Fig. 2(a), the full line is based on the simplified Eqs. (9) and (13), the other used parameters are  $\alpha'=30$ ,  $B'=10^{-2}$ ,  $R'=10$ . The  $t'_e$  is the extraction time given by Eq. (9).

$L' < 1$  and saturates for  $L' > 1$ . The intersection of the linear part and the saturated value can be used for finding a point at which  $L'=1$ .

Note that without the recombination<sup>4</sup>

$$t'_e = (L' - 1)/j' \quad \text{for } L' > 1 \quad (10)$$

and for the monomolecular recombination, controlled by lifetime  $\tau'_g$  (Ref. 4) for  $L' > 1$ ,

$$t'_e = \tau'_g \ln \left[ \frac{L' - 1}{j' \tau'_g} + 1 \right]. \quad (11)$$

There is no saturation of  $t'_{1/2}$ , so that the case of bimolecular recombination can be clearly distinguished. Can we deduce the coefficient of the bimolecular recombination ( $B$ ) from the measured data ( $t'_{1/2}$ )?

Figure 4 displays  $t'_{1/2}$  as a function of  $B'$ , calculated for two values of the detection resistor ( $R'$ ) on the basis of the theory of Sec. III. The positive result is that the  $t'_{1/2}$  value is a sensitive function of  $B'$ . To make the evaluation of  $B'$  from the experimental results practical, we present in the next section a simplified theory, which allowed us to get an analytical expression for  $t_e$  as a function of  $B'$ .

## V. SIMPLIFIED EXPRESSION FOR EXTRACTION TIME

Due to the fact that under the SCLC conditions ( $L' \gg 1$ ) the electric field in the reservoir is screened within a very short time ( $\tau'_0 = 2/L'\alpha'$ ) (Ref. 4) and so the drift of the carriers is interrupted, we can, as a reasonable approximation, separate the time and coordinate dependences of the carrier concentration

$$p'(x', t') = \alpha' P'(t') \exp(-\alpha' x'),$$

where  $P'(t')$  is the total number of photogenerated pairs. When we integrate along the coordinate, the continuity equation for mobile carriers is

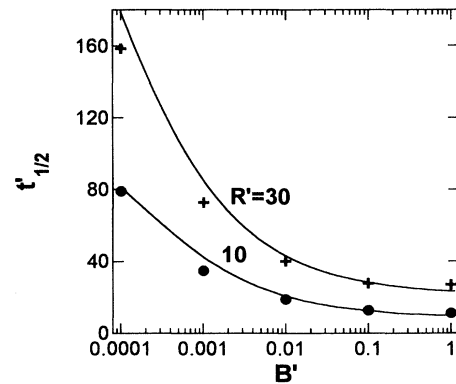


FIG. 4. The SCLC-TOF current pulse half-width ( $t'_{1/2}$ ) as a function of the coefficient of the bimolecular recombination ( $B'$ ) for two values of the detection resistor ( $R'=10$  and  $30$ ). The points are calculated on the basis of the full theory of Sec. III and the full lines according to the simplified Eqs. (9) and (13), both for  $\alpha'=30$ ,  $R'=10$ , and  $L'=10$  (see text).

$$\frac{\partial p'(x', t',)}{\partial t'} = -B' p'(x', t') n'(x', t') - \frac{\partial j'_{pc}(x', t')}{\partial x'}$$

As far as the carriers of opposite sign are immobile [ $j'_c(0, t')=0$ ], we obtain

$$\frac{dp'(t')}{dt'} = -\frac{B'\alpha'P'^2(t')}{2} - j'_c(1, t'). \quad (12)$$

As the charge  $L'=1$ , necessary for the screening of the electric field, within  $\tau'_0 \ll 1$  leaves the reservoir, only the remaining charge  $(L'-1)$  can recombine. By the integration of Eq. (12) from  $t'=0$ , for which  $P'(0)=L'-1$  to  $t'=t'_e$ , where  $P'(t'_e)=0$ , we have obtained for  $L' > 1$

$$t'_e = \sqrt{2/B'\alpha'j'_c} \arctan[(L'-1)\sqrt{B'\alpha'/(2j'_c)}]. \quad (13)$$

For high light intensity ( $L' \gg 1$ ) the extraction time  $t'_e(L')$  saturates and is given as

$$t'_e = \frac{\pi}{\sqrt{2B'\alpha'j'_c}}. \quad (14)$$

Generally the effective sample resistance is a function of voltage and so consequently of time. However, for the purpose of comparing the above simplified expressions with the full theory of Sec. III, we take  $j'_c = 1/(1+R')$ , which is within the limit of the differential ( $j'_c=1$  for  $R' \ll 1$ ) and the integral modes ( $j'_c=1/R'$  for  $R' \gg 1$ ) reasonable approximation.

The comparison of the full theory of Sec. III (points) with the simplified expressions (9), (13), and (14), illustrated by the full lines in Figs. 3, 4, and 5, shows very good agreement. The small quantitative discrepancy of  $t'_e(L')$  around  $L'=1$  (see Fig. 3) is related to the dispersion of the drifting charge induced by a repulsive Coulomb interaction, which is around  $L'=1$  comparable with the applied external field. The small difference of the saturated  $t'_{1/2}$  value can induce a certain difference as concerns the

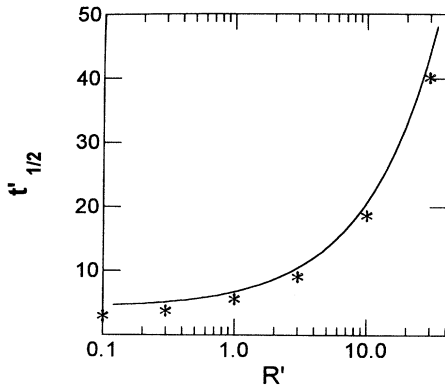


FIG. 5. The SCLC-TOF current pulse half-width ( $t'_{1/2}$ ) as a function of the detection resistor  $R'$  (in normalized units, see text). The points are calculated on the basis of the full theory of Sec. III and the full line according to the simplified Eqs. (9) and (13), both for  $\alpha'=30$ ,  $B'=10^{-2}$ , and  $L'=30$  (see text).

$B'$  value, deduced on the basis of Eq. (14); however, the functional dependence will not be changed. We have found that when the value of  $j'_c$  is deduced from the measured value  $\Delta U'/R'$ , then this difference decreases.

Now we want to comment on a few important points. First, in the case of the Langevin-type recombination ( $B'=1$ ) and differential regime ( $j'_c=1$ )

$$t'_e = \frac{\pi}{\sqrt{2\alpha'}}. \quad (15)$$

This means that for a strongly absorbed light ( $\alpha' \gg 1$ )  $t'_e \rightarrow 0$  for arbitrarily high light intensity; so, it is impossible to create a charge reservoir higher than  $P'=1$  ( $Q=CU$ ). In such a case, we can observe experimentally only a space-charge perturbed ( $P'=1$ ) current transient for  $L' > 1$ . This conclusion was drawn from another reasoning in Ref. 3 and served as a proof of the existence of the Langevin-type recombination in *a*-Se and its absence in *a*-Si:H, where SCLC is found.

Second, the saturation of  $t'_e$  with the increasing  $L'$  can be found only for bimolecular or higher-order recombination. For example, as follows from Eq. (14), in a bimolecular case  $t'_e \approx U'^{-1/2}$  and for an interband Auger recombination  $t'_e \approx U'^{-2/3}$ .

Finally, if both the monomolecular and bimolecular recombinations coexist, the slope of  $t'_e(L')$  dependence and the saturated value of  $t'_{1/2}$  will be lower in comparison with the pure bimolecular case and the resulting expression for

$$t'_e = \frac{2}{\sqrt{2B'\alpha'j'_c - 1/\tau_g'^2}} \arctan \left[ \frac{\sqrt{2B'\alpha'j'_c\tau_g'^2 - 1}}{(2j'_c\tau_g')/(L'-1) + 1} \right] \quad (16)$$

is more complicated.

## VI. EXPERIMENTAL RESULTS AND THEIR DISCUSSION

The experimental results obtained on 50  $\mu\text{m}$  [Fig. 1(b)] and 1  $\mu\text{m}$  [Fig. 2(b)] *a*-Si:H *p-i-n* junctions correspond very well with the SCLC-transient calculated on the basis of the theory of Sec. III in both the differential mode [compare Figs. 1(a) and 1(b)] and the integral mode [compare Figs. 2(a) and 2(b)].

The origin of some of the quantitative differences is clear. For example, the initial (screening) spike in Fig. 1(b) is rather short and small due to the very high absorption coefficient (in normalized units  $\alpha'=500$ ) for the light used in the experiment.

As another example, a slight decrease in the current in the small signal case ( $L' < 1$ ) for  $t < t_{tr}$  [see Fig. 1(b)] contrary to the increase in the theoretical curve [Fig. 1(a)] is clearly due to the volume trapping, present in the experiment.

The clear saturation of  $t'_{1/2}$  with the increasing light intensity  $L'$  [see Fig. 6(a)] together with its appropriate

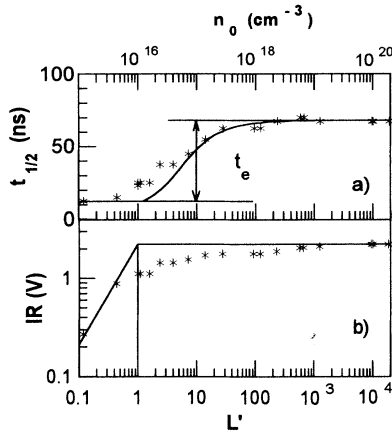


FIG. 6. (a) The half-width ( $t_{1/2}$ —in absolute units) and (b) the magnitude [expressed as the current ( $I$ ) times resistance ( $R$ )] of the SCLC-TOF transient as a function of the normalized light intensity ( $L'$ ) or as a concentration  $n_o$  of the carriers, photogenerated by 2.3-eV light pulse. The results (points) have been measured on a 1- $\mu\text{m}$ -thick  $a\text{-Si:H}$   $p\text{-i-n}$  junction at 1.5-V applied voltage, 300 K on  $R=50\text{-}\Omega$  resistor. The full line was calculated according to Eq. (13) with  $B=4.3\times 10^{-10}\text{ cm}^3/\text{s}$ .

voltage and absorption coefficient dependencies for both  $\alpha=10^5\text{ cm}^{-1}$  (for 2.3-eV light) and  $\alpha=10^6\text{ cm}^{-1}$  (for 3.45-eV light) represent clear proof of the existence of the bimolecular recombination for the generated carrier density  $n_o > 3\times 10^{17}\text{ cm}^{-3}$ .

The values of the bimolecular-recombination coefficient  $B$ , which were obtained for our different samples from the saturated values of the extraction time ( $t_e'$ )

according to Eqs. (9) and (14) are presented in Table I. We also obtained a similar  $B$  value from the hole extraction time measurements.<sup>12</sup> Our obtained values are an order of magnitude smaller than  $B$  obtained from the optical measurements (see Table I). In obtaining the  $B$  value, we have used an approximate formula (14) and also the same value of  $\alpha$  for all samples; however, the inaccuracy thus introduced is much less than an order of magnitude difference between our results and the results of optical measurements. Also, the photogenerated charge carrier density ( $n_o$ ), at which the bimolecular recombination starts, and the monomolecular-recombination probability ( $\tau_g^{-1}$ ) based on our results are substantially smaller. There arises a question of how to explain these differences.

One possible explanation is that by the high-repetition rate pulsed illumination  $a\text{-Si:H}$  can degrade and so the difference of  $B$  values is related to the different stages of degradation. To test this idea, we have degraded a 1- $\mu\text{m}$ -thick  $a\text{-Si:H}$   $p\text{-i-n}$  junction by 1-A/ $\text{cm}^2$  forward current. From the charge collection of the small signal TOF, we found that by this degradation the deep trapping  $(\mu\tau)_D$  product, related to the midgap density of states (DOS), decreased approximately four times.

In Fig. 7 we show  $t_{1/2}$  (in ns as the absolute units) as a function of the normalized light intensity ( $L'$ ) for the annealed (“\*”) and degraded (“o”) state. From Ref. 5, it is clear that the degradation-induced increase in the DOS decreased both the volume deep trapping and the monomolecular-recombination time in the reservoir region. Full lines in Fig. 7 illustrate the fit based on Eq. (16) for the annealed state ( $B=7\times 10^{-10}\text{ cm}^3/\text{s}$ ,  $\tau_g=120$  ns) and for the degraded states where in one case we have

TABLE I. Summary of the absolute (not normalized) values of the bimolecular recombination coefficient ( $B$ ) and starting concentration of the bimolecular recombination ( $n_o$ );  $d$ -sample thickness.

Source of samples or values	$d$ , $\mu\text{m}$	$B$ , $10^{-9}\text{ cm}^3/\text{s}$	$n_o$ $10^{17}\text{ cm}^{-3}$
<i>Photoelectrical measurements:</i>			
University of Neuchatel, Switzerland	0.4 50.0	0.6 0.46	<3
Siemens, Munich, Germany	1.0	0.43	$\sim 1$
Before degradation	2.0	0.64	1.5
$N_{\text{DOS}}=0.8\times 10^{16}\text{ cm}^{-3}$			
After degradation		0.64	
$N_{\text{DOS}}=3\times 10^{16}\text{ cm}^{-3}$ (Estimated from reverse current)			
For holes ( $T=339\text{ K}$ )	5.0	$\sim 1$	$\sim 1$
<i>ENEA-CRIF, Portici, Italy</i>			
Before degradation	1.0	0.7	<4
After degradation (7 h by 1-A/ $\text{cm}^2$ forward current)		0.7	$\sim 8$
Haffer and Kunst (Ref. 13)		1	3
<i>Optical measurements:</i>			
Fauchet <i>et al.</i> (Ref. 6)		26	50
Esser <i>et al.</i> (Ref. 9)		7	100
Vanderhaghen <i>et al.</i> (Ref. 10)		3	200
Devlen <i>et al.</i> (Ref. 11)		2	8

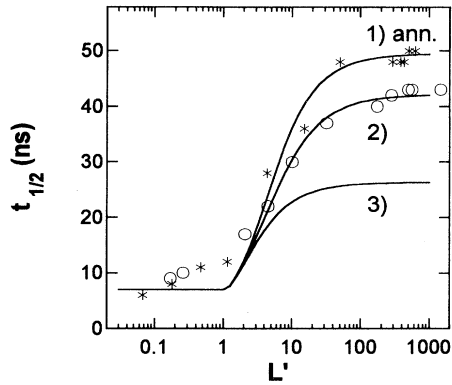


FIG. 7. The SCLC-TOF current pulse half-width ( $t_{1/2}$ —in absolute units) as a function of the normalized light intensity ( $L'$ ), obtained on a 1- $\mu\text{m}$ -thick  $a\text{-Si:H}$   $p\text{-i-n}$  junction in the annealed state (“\*”) and partially degraded state (“o”). The full lines are calculated curves according to Eq. (16). The parameters found by the best fit of curve 1 are  $B = 7 \times 10^{-10} \text{ cm}^3/\text{s}$  and  $\tau_g = 120 \text{ ns}$ ; for curve 2, the  $\tau_g$  was four times reduced to 30 ns and  $B$  kept constant; for curve 3, in addition to the fourfold reduction of the  $\tau_g$ , the  $B$  value has been four times increased to  $B = 2.8 \times 10^{-9} \text{ cm}^3/\text{s}$  (see text).

decreased only the monomolecular lifetime  $\tau_g$  four times to  $\tau_g = 30 \text{ ns}$  and did not change the bimolecular coefficient  $B$ . In the other case both the monomolecular- and bimolecular-recombination parameters have been changed (after degradation  $\tau_g = 30 \text{ ns}$  and  $B = 2.8 \times 10^{-9} \text{ cm}^3/\text{s}$ ). It is evident that the good fit can be obtained only when we assume that the degradation-induced midgap deep states change only the monomolecular- and not the bimolecular-recombination parameters (see also Ref. 14).

Note that the difference between the experimental values of  $t_{1/2}$  and the simplified theory in the region  $L \leq 1$  is caused by the spread of the drifting charge sheet (see Sec. V), which was not taken into account by the simplified theory. Note also that for the nondegraded samples, the  $t_{1/2}$  value saturation is mainly determined by  $B$  [see Eq. (16)]. Therefore, degradation is not the main reason for the differences between the values of  $B$  and bimolecular recombination starting concentrations  $n_0$  measured optically and photoelectrically.

In the case of optical measurements, it is difficult to distinguish between the losses of the free carriers by trapping and by recombination; in our case, we extract also the shallow trapped carriers. We believe that the differences are caused by the fact that the recombination observed in optical experiments occurs before electron trapping into the band tail; in our photoelectrical experiment, recombination after shallow trapping is also included. This is supported by the experimental finding that both  $B$  and  $\mu$  deduced from photoelectrical measurements depend on temperature in the same way (see Fig. 8) contrary to the optical measurement, which give  $B$  independent of temperature.<sup>10</sup> Our measurements were made at  $T > 290 \text{ K}$ . At lower temperatures due to the strong temperature dependence of the mobility, there are problems with the fulfillment of the conditions of the in-

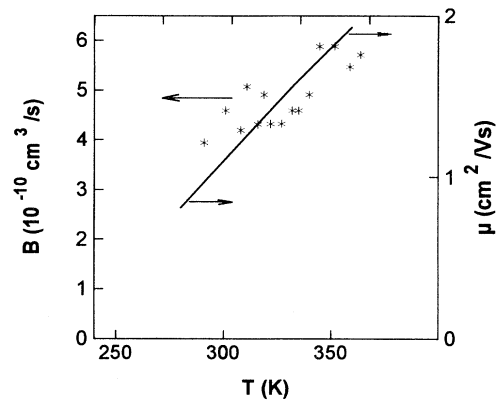


FIG. 8. The temperature dependence of the bimolecular-recombination coefficient  $B$ , obtained on the basis of the simplified expressions (9) and (13) from the measurements of the extraction time on a 1- $\mu\text{m}$ -thick  $a\text{-Si:H}$   $p\text{-i-n}$  junction. The full line, the temperature dependence of  $a\text{-Si:H}$  electron drift mobility, is shown for comparison (see text).

tegral mode. This, together with the increasing dispersion of carriers, makes the finding of the precise  $B$  values difficult.

From the above considerations, we can draw the following conclusions.

(i) The bimolecular recombination extends up to the ns time region (see also Ref. 13).

(ii) The bimolecular recombination proceeds between a free electron and a localized hole (recombination is controlled by the mobility of electrons), because practically all holes are trapped before 10-ns time.

(iii) The parameters  $B$  and  $\tau$  deduced from photoelectrical measurement have to be normalized by inverse of the shallow trapping factor  $f = \mu/\mu_0 = n/n_0$ , where  $n_0$  is the photogenerated carrier concentration,  $n$  is the (remaining) free-carrier concentration, and  $\mu$  and  $\mu_0$  are the drift and microscopic mobilities, respectively. In this case, the true bimolecular-recombination coefficient (not influenced by shallow trapping) is  $B_0 = B\mu_0/\mu$ . For  $T = 300 \text{ K}$  and at low electrical field, the factor  $\mu_0/\mu \approx 10$  and the optically and photoelectrically deduced  $B$  (corrected  $B_0$ ) reasonably agree.

The fact that the microscopic origin of the fast bimolecular recombination is still unknown is a serious principal problem. As follows from this work and the other published results, the bimolecular recombination extends in the concentration interval  $10^{17} - 10^{21} \text{ cm}^{-3}$  and in the time interval from nanoseconds to subpicoseconds. Can we put forward a model that would explain all experimental data?

First, the absence of the room-temperature photoluminescence together with other arguments<sup>6,9</sup> give clear proof that the bimolecular recombination is a nonradiative process. Moreover, the small observed values of the bimolecular-recombination coefficient  $B$  in comparison with the predicted one for the Langevin-type recombination  $B_L = e\mu/\epsilon\epsilon_0 = 1.6 \times 10^{-7} \text{ cm}^3/\text{s}$  for  $\mu = 1 \text{ cm}^2/\text{Vs}$  clearly exclude this possibility (see also Ref. 4). The multiphonon processes, especially sequential phonon emis-

sion, cannot explain the bimolecular recombination because at short time (0.4 ps) and high light intensity (carrier concentration  $n_o \approx 10^{21} \text{ cm}^{-3}$ ) the phonon frequency and density of localized states are too low.<sup>6</sup>

It is possible that the bimolecular recombination proceeds via light-induced, short-living (not relaxed) states,<sup>15,16</sup> the concentration of which is a function of the light intensity. To test this hypothesis we performed an experiment, described in Fig. 9, in which we compared  $t'_{1/2}$  (a) deduced from the small signal case (controlled by the monomolecular recombination), and  $t'_{1/2}$  (c) (see Fig. 9), deduced from the small signal case to which the large intensity pulse (b) from the bimolecular region ( $n_o > 10^{18} \text{ cm}^{-3}$ , see Fig. 6) proceeded with a certain time interval ( $t_{\text{del}}$ ).

If the large intensity pulse (b) induced the short-living states, the test pulse width in the case (c),  $t'_{1/2}$  (c) should be shorter than  $t'_{1/2}$  (a). The experimental results have shown that  $t'_{1/2}$  (a) =  $t'_{1/2}$  (c) within the experimental error for  $t_{\text{del}}$  in the range 200 ns–1  $\mu\text{s}$ ; therefore, evidence for short-living states has not been found.

It was suggested that the bimolecular recombination can be explained by an Auger-type recombination of highly correlated electron-hole pairs<sup>9</sup> or of two free and one trapped charge carriers.<sup>7</sup>

However, the Auger-type recombination has been questioned in Ref. 6 owing to the absence of the delay between the carrier recombination and the lattice heating, which should be associated with the cooling of very hot carriers produced in any Auger recombination.

We believe that the Auger recombination is still the most probable mechanism because it represents the quickest way of the nonradiative loss of energy. In Ref. 7, we have suggested the model of the Auger recombination of the two free and one trapped charge carriers. Such a process is more probable than the interaction of three free particles because the impulse-conservation law need not be fulfilled. For such a process, the kinetic equation for the electrons is

$$\frac{\partial n}{\partial t} = -\gamma_n n p (N_t - n_t),$$

where  $N_t$  is the density of localized states and  $n_t$  is the concentration of electrons trapped in these states.

If the trapping of holes is quicker than the trapping of electrons (as supported by a wider valence-band tail), then for  $n = p > N_t$

$$\frac{dn}{dt} = -\gamma_n N_t n^2, \quad (17)$$

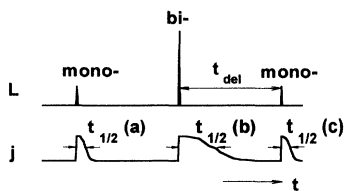


FIG. 9. The schematic picture illustrating the special TOF experiment, performed for the detection of the short-living states created by the high intensity light pulse (see text).

which corresponds to the bimolecular character of the recombination with the bimolecular-recombination coefficient  $B = \gamma_n N_t$ .

As the bimolecular recombination prevails for  $n_o > 3 \times 10^{17} \text{ cm}^{-3}$  of the photogenerated carriers, the concentration of the localized states, occupied by holes that control the bimolecular recombination, has to be  $N_t < 3 \times 10^{17} \text{ cm}^{-3}$ . If we take this value of  $N_t$ , we obtain the coefficient  $\gamma_n = B/N_t = 10^{-26} \text{ cm}^6/\text{s}$ , the fully realistic value for this type of recombination.<sup>17</sup>

In our model the deep valence-band-tail states act as the  $N_t$  centers; during the Auger process, the hole trapped at  $N_t$  is excited into the valence band. The absence of the delay between the lattice heating and the excitation, observed in Ref. 6, could be explained if the thermalization speed is higher for holes than for electrons. Note that the observed value of 1 eV/ps (Ref. 6) is related to the electron thermalization if the densities of extended states  $N_c(E) < N_v(E)$  so that the energy of the photoexcited electrons is higher than for the corresponding holes.

In other words, our model is able to explain the observed experimental results but further experiments are necessary to obtain clear proof. There exists another alternative mentioned in Ref. 6—the recombination between the free carriers where the gained energy is transferred to a few “optical” or “local” vibrations of the Si-H bond at the same time.

## VII. CONCLUSIONS

We can summarize the above results as follows.

(i) We have presented a detailed theory of the SCLC-TOF transients induced by an instantaneous pulse of light in which in addition to the realistic absorption profile we have taken into account the bimolecular recombination in the reservoir region and the value of the detection resistor.

(ii) We have developed a simplified theory that has allowed us to find the analytical relation between the extraction time ( $t_e$ ) and the coefficient of the bimolecular recombination ( $B$ ). We have verified good agreement between the simplified and full theory, and the experimental results.

(iii) On the basis of the experimental results on *a*-Si:H, we have discussed the possible microscopic models of the bimolecular recombination in this material and presented our model, based on the Auger process of two free and one trapped carrier. As indicated by our ns time photoelectrical measurements and the optical measurements by the pump-and-probe technique in the ps time region, we believe that the nature of the recombination in *a*-Si:H is the same in the ps-ns region and the difference in  $B$  values has been explained by the shallow trapping.

## ACKNOWLEDGMENTS

The authors would like to acknowledge the supply of *a*-Si:H samples (*p-i-n* diodes) by A. Shah (Neuchatel), M. Hoheisel (Munich), and G. Conte (Portici), and the partial support of EC Grant No. PECO-3209.



- <sup>1</sup>J. Kočka, O. Klíma, G. Juška, M. Hoheisel, and R. Plattner, *J. Non-Cryst. Solids* **137-138**, 427 (1991).
- <sup>2</sup>M. Simhony and J. Gorelik, *J. Phys. Chem. Solids* **26**, 1133 (1965).
- <sup>3</sup>G. Juška, *Lithuanian Phys. J.* **30**, 58 (1990).
- <sup>4</sup>G. Juška, M. Viliunas, O. Klíma, E. Šípek, and J. Kočka, *Philos. Mag. B* **69**, 277 (1994).
- <sup>5</sup>J. Kočka, G. Juška, O. Klíma, E. Šípek, G. Nobile, E. Terzini, and G. Conte, *J. Non-Cryst. Solids* **164-166**, 489 (1993).
- <sup>6</sup>P. M. Fouchet, D. Hulin, R. Vanderhaghen, A. Mourchid, and W. L. Nighan, Jr., *J. Non-Cryst. Solids* **141**, 76 (1992).
- <sup>7</sup>G. Juška, J. Kočka, M. Viliunas, and K. Arlauskas, *J. Non-Cryst. Solids* **164-166**, 579 (1993).
- <sup>8</sup>K. C. Kao and H. Hwang, *Electrical Transport in Solids* (Pergamon, Oxford, 1981).
- <sup>9</sup>A. Esser, K. Seibert, H. Kurz, G. N. Parisons, C. Wang, B. N. Davidson, G. Lucovsky, and R. J. Nemanich, *J. Non-Cryst. Solids* **11**, 573 (1989); *Phys. Rev. B* **41**, 2879 (1990).
- <sup>10</sup>R. Vanderhaghen, A. Mourchid, D. Hulin, D. A. Yong, W. L. Nighan, and P. M. Fauchet, *J. Non-Cryst. Solids* **137-138**, 543 (1991).
- <sup>11</sup>R. I. Devlen, G. S. Kanner, Z. Vardeny, and J. Tauc, *Solid State Commun.* **78**, 665 (1991).
- <sup>12</sup>G. Juška, M. Viliunas, S. Vengris, A. Fejfar, and J. Kočka, in *Proceedings of the Eighth International School on Condensed Matter Physics* (Taylor & Francis, London, 1994).
- <sup>13</sup>C. M. Haffer and M. Kunst, *Chem. Phys. Lett.* **211**, 203 (1993).
- <sup>14</sup>R. Vanderhaghen, R. Amokrane, D. Han, and M. Silver, *J. Non-Cryst. Solids* **164-166**, 599 (1993).
- <sup>15</sup>T. M. Leen and J. D. Cohen, *J. Non-Cryst. Solids* **137-138**, 319 (1991).
- <sup>16</sup>M. Stutzmann, J. Nunnenkamp, M. S. Brandt, and A. Asano, *Phys. Rev. Lett.* **67**, 2347 (1991).
- <sup>17</sup>P. T. Landsberg, *Phys. Status Solidi* **41**, 457 (1970).